

X-ray crystal structures of transforming p21 ras mutants suggest a transition-state stabilization mechanism for GTP hydrolysis

GILBERT G. PRIVÉ*†, MICHAEL V. MILBURN*‡, LIANG TONG*§, ABRAHAM M. DEVOS*¶, ZIRO YAMAIZUMI||, SUSUMU NISHIMURA||, AND SUNG-HOU KIM*·**

*Department of Chemistry and Lawrence Berkeley Laboratory, University of California, Berkeley, CA 94720; and ||National Cancer Center Research Institute, Tokyo, Japan

Communicated by Melvin Colvin, December 9, 1991 (received for review September 16, 1991)

ABSTRACT *RAS* genes isolated from human tumors often have mutations at positions corresponding to amino acid 12 or 61 of the encoded protein (p21), while retroviral *ras*-encoded p21 contains substitutions at both positions 12 and 59. These mutant proteins are deficient in their GTP hydrolysis activity, and this loss of activity is linked to their transforming potential. The crystal structures of the mutant proteins are presented here as either GDP-bound or GTP-analogue-bound complexes. Based on these structures, a mechanism for the p21 GTPase reaction is proposed that is consistent with the observed structural and biochemical data. The central feature of this mechanism is a specific stabilization complex formed between the Gln-61 side-chain and the pentavalent γ -phosphate of the GTP transition state. Amino acids other than glutamine at position 61 cannot stabilize the transition state, and amino acids larger than glycine at position 12 would interfere with the transition-state complex. Thr-59 disrupts the normal position of residue 61, thus preventing its participation in the transition-state complex.

ras-encoded proteins (p21) play a pivotal role in the signaling of cell growth and differentiation. p21 communicates in its GTP-bound state to effector proteins and is deactivated by hydrolysis of GTP to GDP (reviewed in refs. 1–3). The p21 proteins possess an inherent GTPase activity that is stimulated *in vivo* by GAP (GTPase-activating protein) (4–6) and by the GAP-related domain of the neurofibromatosis type 1 protein (NF1) (7, 8). The molecular switching from the GDP-bound to the GTP-bound form is accompanied by extensive conformational changes in two parts of the protein, the switch I and switch II regions (Fig. 1).

Several transforming *ras* genes have been found. *RAS* oncogenes isolated from human tumor cells often have single point mutations in the codons corresponding to amino acid position 12, 13, 61, or 146 (1, 9). Both Harvey and Kirsten rat sarcoma viruses have a *ras* gene with mutations at codons 12 and 59, and *in vitro* mutagenesis at position 12, 13, 59, 61, 63, 116, 117, or 119 endows p21 with cell-transforming capabilities (1–3). These positions make up part of the guanine nucleotide-binding pocket (10–12), and these can be mapped to either the phosphate region (positions 12, 13, 59, 61, and 63) or base region (positions 116, 117, 119, and 146) (Fig. 1). To date, all of the biochemically characterized phosphate-region mutants show a decrease in the intrinsic GTP hydrolysis rate and are insensitive to GAP and the GAP-related domain of NF1 stimulation. In addition, all of the base-region mutations (and several of the phosphate-region mutations) that have been tested show a decreased affinity for the guanine nucleotide. Either or both of these properties—reduced hydrolysis rates and weakened nucleotide binding—are thought to be the biochemical reasons for cell transformation by oncogenic p21 proteins.

To understand the structural basis for the reduction in GTPase activity by the phosphate-region mutants, we have analyzed the conformational differences between the crystal structures of normal and mutant proteins,^{††} paying special attention to distinguish structural changes due to amino acid substitutions from those due to crystal packing.

Based on the crystal structures of these mutant and wild-type proteins, we propose a transition-state stabilization mechanism for GTP hydrolysis by p21. This new mechanism differs from a water-activation mechanism (13) and provides a rationale for the transforming effects of mutations at positions 12, 59, and 61. Our structural interpretations of the oncogenic mutations at residues 12 and 61 are different from a previously published analysis (14), and that for residue 59 is new.

METHODS

The expression, purification, and crystallization of both the GDP and GDP-[CH₂]P complexes with *c-Ha-ras*-encoded p21 have been described (15, 16). Unless specified otherwise, a truncated form of p21 [p21-(1–171)] was used to form the complexes (see Table 1). Data for the p21·GDP, p21(G12V)·GDP, p21(Q61L)·GDP, and p21(A59T)·GDP crystals were collected at the Stanford Synchrotron Research Laboratory on x-ray film and then processed and reduced as described (17). The p21(G12V, A59T)·GDP, p21·GDP-[CH₂]P, and p21(Q61L)·GDP-[CH₂]P diffraction data were collected on type-II Fuji imaging plates at the Photon Factory synchrotron in Tsukuba, Japan, on a screenless Weissenberg camera modified for protein crystallography (18). The plates were read on a Fuji BA-100 scanner by using a 100- μ m raster size. The raw images were then reduced to structure factors by using the program WEIS (19). $R_{\text{merge}}(I)$ values (19) were all below 7.5%.

All of the mutant structures were solved by using the structure of the normal p21·GDP or p21·GDP-[CH₂]P complexes excluding the regions surrounding the mutation sites. Crystallographic refinement was carried out with a combination of the X-PLOR (20) and TNT programs (21). Deleted regions of the protein were built into difference electron density towards the final stages of the refinement.

Abbreviations: GDP-[CH₂]P, guanosine 5'-[β , γ -methylene]triphosphate; GDP-[NH]P, guanosine 5'-[β , γ -imido]triphosphate; GAP, GTPase-activating protein; NF1, neurofibromatosis type 1.

[†]Present address: Molecular Biology Institute, University of California, Los Angeles, CA 90024-1570.

[‡]Present address: Department of Structural and Biophysical Chemistry, Glaxo, Inc., 5 Moore Drive, Research Triangle Park, NC 27790.

[§]Present address: Department of Biological Sciences, Purdue University, Lafayette, IN 47906.

[¶]Present address: Department of Protein Engineering, Genentech, Inc., South San Francisco, CA 94080.

^{**}To whom reprint requests should be addressed.

^{††}The atomic coordinates and structure factors have been deposited in the Protein Data Bank, Chemistry Department, Brookhaven National Laboratory, Upton, NY 11973 {reference R6P21SF (*c-Ha-ras* p21·GDP), R7P21SF [p21(G12V)·GDP], and R8P21SF (p21·GDP-[CH₂]P)}.

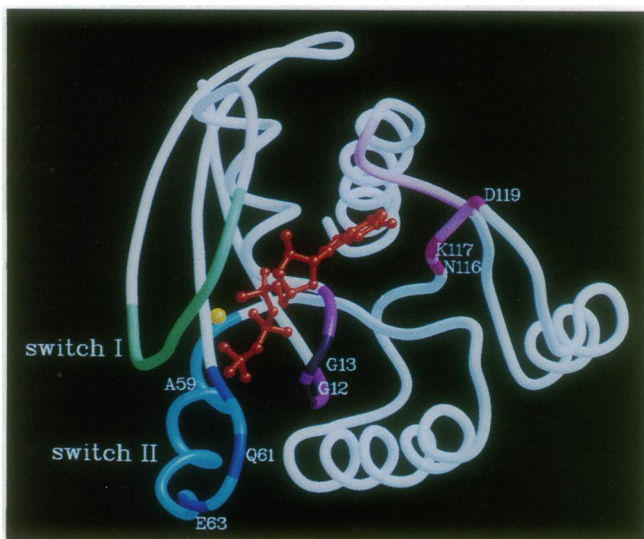


FIG. 1. View into the nucleotide-binding pocket of p21. The GTP is shown in red (base at top, phosphates at bottom), and the Mg^{2+} ion is in yellow. The phosphate-binding loop is light purple (residues 10–17, residues 10–14 from loop L1, and part of the α_1 -helix), the switch I region is light green [residues 30–38 (residues 30–37 from loop L2 and part of the β_2 -strand)], the switch II region is light blue [residues 60–76 (residues 60–66 from loop L4 and a part of the α_2 -helix)], and the base-recognition regions are light pink (residues 116–119 and 143–147). The locations of specific residues are shown in the darker colors. Oncogenic mutation positions 12, 13, 59, 61, and 63 cluster near the phosphates, and positions 116, 117, and 119 are located near the guanine base.

RESULTS AND DISCUSSION

Gln-61 Is Not Essential for Positioning the Attacking Water Molecule in GTP Hydrolysis. Replacement of the normal Gln-61 with 17 other amino acids reduces intrinsic GTPase activity of p21 (22). All of these except the proline and glutamate mutants have transforming activity. The crystal structure of the GDP-bound p21(Q61L) mutant at 2.3 Å resolution shows little structural difference from that of normal p21, including disorder in the region of residues 60–67. Similar disordering has been reported in a guanosine 5'-[β , γ -imido]triphosphate (GDP-[NH]P) complex of p21 as well, where the molecule shows multiple conformations in

the region of residues 61–64 for both the normal (13) and mutant (14) structures. However, in the GDP-[CH₂]P-bound p21(Q61L) crystal structure, where there are four independent molecules per asymmetric unit (Table 1), one of the four molecules shows strong and easily interpretable density for this region of the protein (Fig. 2) and has an average temperature factor of 19 Å² for residues 59–66. Similarly, one of the four independent molecules in the normal GDP-[CH₂]P-bound p21 crystal structure is well ordered in this same region. In three of the molecules, the average main-chain temperature factors of residues 59–66 is about 62 Å² but only 29 Å² in the fourth molecule, only slightly higher than other well-defined regions of the protein.

The GTP hydrolysis reaction of p21 has been shown to proceed via a direct attack of a water molecule to the GTP γ -phosphate (23), and this requires an attacking water molecule that is roughly in line with the scissile γ -P—O bond. We have located strong electron density for such a water molecule in all four independent molecules of the normal p21-GDP-[CH₂]P structure (Fig. 2 Upper), although the molecules have weak electron density in the region of residues 60–64 of the protein. A water molecule at a similar position has been described in the GDP-[NH]P structure (13), which has a single molecule in the asymmetric unit.

In the 2.0-Å structure of p21(Q61L)-GDP-[NH]P by Krenzel *et al.* (14), the leucine side chain occupies a position different from that of the "active" glutamine in the normal structure. In contrast, the Leu-61 side chain in our best resolved p21(Q61L)-GDP-[CH₂]P molecule has a side-chain orientation essentially the same as in our normal Gln-61 structure and also has the in-line water at the same position (Fig. 2 Lower). A surprising finding, thus, is that an equivalent water molecule is found in all four of the normal p21 structures and at least two of the four mutant p21(Q61L) structures, although the four molecules in each case are in different crystal environments and have different loop L4 conformations. This observation directly implies that Gln-61 is not required to fix this water molecule at the attacking position. Rather, this water molecule is tightly bound and presumably activated by strong interactions with the γ -phosphate and the main-chain carbonyl group of Thr-35.

Transition-State Stabilization Mechanism for GTP Hydrolysis. Previously, a mechanism for p21-catalyzed GTP hydrolysis has been proposed in which Gln-61, in a hydrogen-

Table 1. Refinement statistics for p21 mutants

Protein complex*	Space group	Unit cell	N^\dagger	Total Refls	Resolution, Å	R factor, %	rms bond, Å	rms angle, deg
p21-GDP	$P6_522$	$a = b = 83.2, c = 105.1$ $\alpha = \beta = 90.0, \gamma = 120.0$	1	8,566	2.2	18.8	0.026	2.6
p21(G12V)-GDP	$P6_522$	$a = b = 83.2, c = 105.1$ $\alpha = \beta = 90.0, \gamma = 120.0$	1	8,690	2.2	19.2	0.024	2.5
p21(Q61L)-GDP	$P6_522$	$a = b = 83.2, c = 105.1$ $\alpha = \beta = 90.0, \gamma = 120.0$	1	9,447	2.3	20.7	0.027	2.9
p21(A59T)-GDP	$P6_522$	$a = b = 83.3, c = 104.6$ $\alpha = \beta = 90.0, \gamma = 120.0$	1	5,640	2.7	18.4	0.027	2.9
p21(G12V, A59T)-GDP	$P6_522$	$a = b = 82.9, c = 101.8$ $\alpha = \beta = 90.0, \gamma = 120.0$	1	8,160	2.2	21.3	0.021	2.6
Intact p21-GDP	$I4$	$a = b = 97.8, c = 41.8$ $\alpha = \beta = \gamma = 90.0$	1	10,167	2.0	19.5	0.019	2.4
p21-GDP-[CH ₂]P	$P2_1$	$a = 42.0, b = 79.9, c = 130.5$ $\alpha = \beta = 90.0, \gamma = 117.5$	4	41,345	1.95	18.8	0.014	2.6
p21(Q61L)-GDP-[CH ₂]P	$P2_1$	$a = 42.0, b = 79.9, c = 129.2$ $\alpha = \beta = 90.0, \gamma = 117.5$	4	31,061	2.00	20.3	0.019	3.6

*All structures are with the truncated p21 "catalytic domain" fragment, p21-(1–171), except for "Intact p21-GDP" (p21 residues 1–188). Mutations are shown in single letter code: G12V indicates the Gly-12 → Val mutation, Q61L indicates the Gln-61 → Leu mutation, and A59T indicates the Ala-59 → Thr mutation. GDP-[CH₂]P, guanosine 5'-[β , γ -methylene]triphosphate. Refls, reflections.

† Number of crystallographically independent molecules.

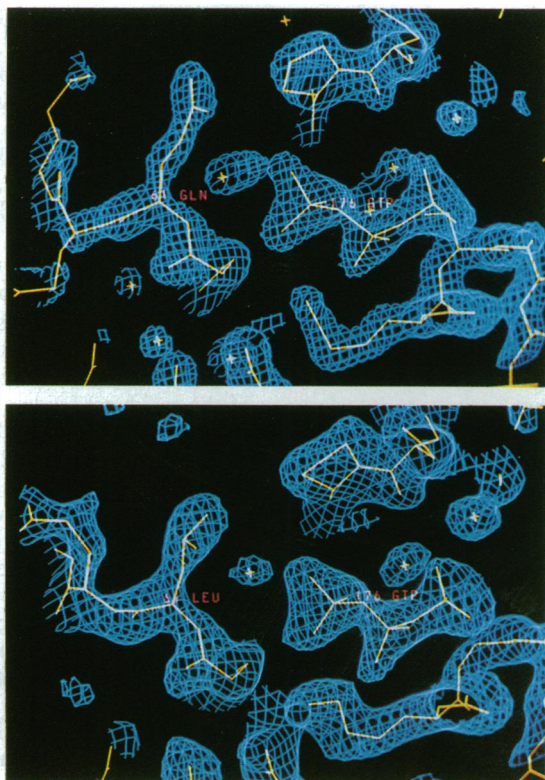


FIG. 2. (Upper) $2F_o - F_c$ electron density of one of the four independent molecules (molecule C) in the L4 region of normal p21, showing the Gln-61 side chain, the GDP-[CH₂]P phosphates, and the in-line water molecule. (Lower) Electron density for molecule C of the p21(Q61L) mutant.

bonded network with Glu-63, activates the in-line water molecule for nucleophilic attack (13). We argue that the activation of the in-line water molecule by Gln-61 is not the rate-limiting step in the hydrolysis reaction for several reasons. (i) All p21 mutants containing amino acid substitutions at position 61 have roughly the same 90% decrease in GTPase activity relative to the normal Gln-61-containing p21 (22). In particular, both p21(Q61E) (Gln-61 → Glu) and p21(Q61H) (Gln-61 → His) have virtually the same low hydrolysis activity as p21(Q61L), even though glutamate or histidine would provide better water-activating groups than the normal glutamine. (ii) Glu-63 is not highly conserved among the

ras-related proteins, although Gln-61 and Glu-62 are seen in almost all of the small GTPase proteins (24, 25). Furthermore, in the ras-related protein RAP1A, in which position 61 is a threonine and position 63 is a glutamine, replacement of Thr-61 with glutamine (while keeping Gln-63) produces a protein with a similar GTP hydrolysis rate as that of normal p21, whereas normal RAP1A has a much lower intrinsic GTPase activity than that of p21 (26). This argues against the direct involvement of Glu-63 in a hydrogen-bonded relay mechanism. (iii) The water-activating ability of Gln-61 is likely to be insignificant compared with that of the γ -phosphate, since glutamine is a poor general base. (iv) The same water molecule was found in all four crystallographically independent molecules of normal p21-GDP-[CH₂]P and at least two of four mutant p21(Q61L)-GDP-[CH₂]P structures, even though the position of the residue 61 side chain is different in each molecule.

The binding pocket surrounding the phosphates is lined with positive charges, and this leads to the electrostatic stabilization of the GTP phosphates. The β - and γ -phosphates form ionic interactions with the Mg^{2+} and the Lys-16 ϵ -amino group and form hydrogen bonds with the main-chain amides of residues 13–17, 35, and 60. This extensive charge neutralization is likely to serve both to fix the flexible phosphate groups in a defined conformation and to reduce the charge density at the γ -phosphorus atom. p21 then act as a catalyst by lowering the activation energy required to reach the transition state. Therefore, we propose that the role of Gln-61 is to reduce the activation barrier by stabilizing the pentavalent phosphate intermediate of the hydrolysis reaction (Fig. 3 Left). The stabilization energy from the two proposed hydrogen bonds between Gln-61 and the transition-state phosphate oxygens are sufficient to explain the rate enhancement of normal p21 relative to the position 61 mutants, which are unable to form this specific complex.

A model of the transition state was built and energy-minimized with molecular dynamics (27), and the resultant complex is shown in Fig. 3 Right. The Gln-61 side chain, which is initially behind the attacking water and the phosphates, moves alongside the γ -phosphate to form hydrogen bonds with the phosphate oxygens (compare Fig. 2 Upper with Fig. 3 Right). The model building involved changes in the conformation of residues 61–63 (the α -carbon positions moved by about 0.5–1 Å and the δ -carbon of Gln-61 moved by about 2.5 Å). This covers the exposed patch at the surface of p21 in the preattack complex, where the GTP γ -phosphate

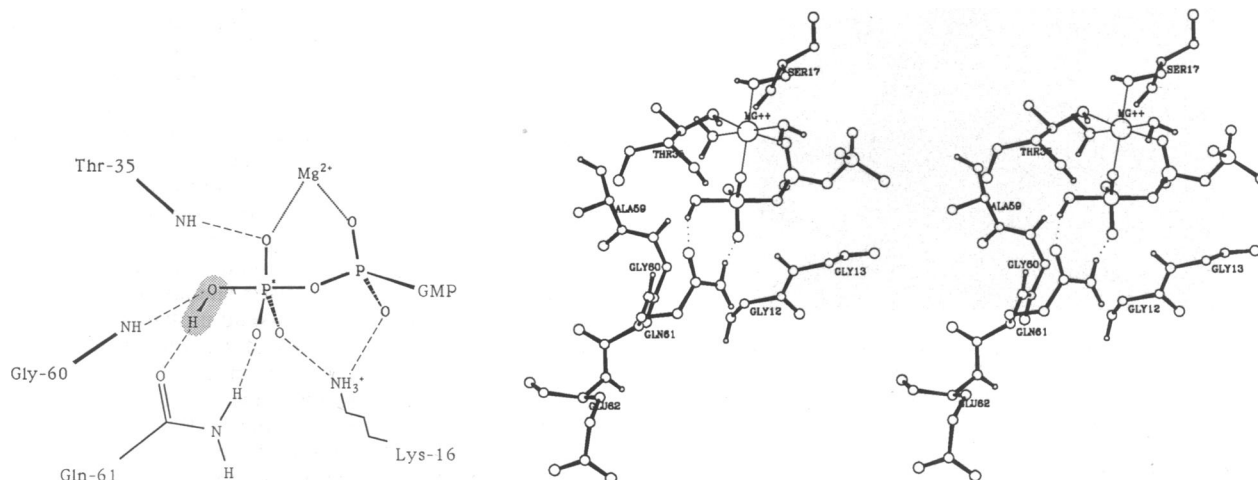


FIG. 3. (Left) Schematic drawing of the transition state of the hydrolysis reaction stabilized by Gln-61. The shaded group indicates the incoming water after attack and loss of a proton. The pentavalent phosphorus is shown by P*. (Right) Energy-minimized model of the p21 transition state. Hydrogen atoms bound to oxygens and nitrogens were included in the energy calculations.

is accessible to solvent (Fig. 4). The side chain of Gln-61 in the transition-state complex is near the α -carbon of Gly-12, the main-chain carbonyl of amino acid 35, and the hydroxyl of Tyr-32, which is in a similar position in three of the four molecules in the crystal structures of both the normal p21-GDP-[CH₂]P and the mutant p21(Q61L)-GDP-[CH₂]P complexes. A model built with asparagine (the other amino acid with the same functional groups as glutamine) at position 61 suggests that perhaps the Gln-61 \rightarrow Asn mutant is deficient in its GTPase activity because the shorter asparagine side chain does not have enough "reach" to interact with the transition state.

Mutations at Position 12 Interfere with the Formation of the Transition State. Replacement of Gly-12 with any amino acid except proline was found to generate transforming mutants (28), and of the mutants that have been tested, all have reduced intrinsic GTPase activity. The overall structures of the GDP-bound form of the normal p21 and the Gly-12 \rightarrow Val mutant [p21(G12V)] are identical except for residues 61–65 of the loop L4 region, which is flexible and has less well-defined electron density than the rest of the protein. The region around the mutation site (residues 10–17 in loop L1) is well ordered in both the normal protein and the mutant, with temperature factors around 20 Å², comparable to that of other well-defined secondary structures of the protein. Surprisingly, the region around the mutation site does not show any significant changes apart from the added Val-12 side chain (17).

The phosphate-binding L1 region in the normal GDP-[CH₂]P structure also shows little difference in conformation when compared with that of the GDP complex. Therefore, we

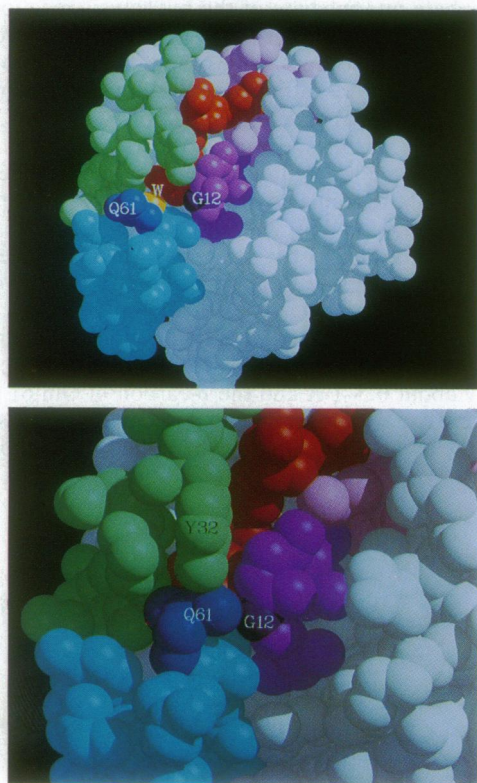


FIG. 4. (Upper) Space-filling representation of p21 in the pre-attack complex, as seen in the GDP-[CH₂]P complex structure. The color scheme is the same as in Fig. 1, except that the attacking water is yellow (note that the Mg²⁺ is buried and is not visible), and only the α -carbon of Gly-12 and the side chain of Gln-61 are shown in the darker colors. (Lower) Close-up view (same orientation as in Upper) of the phosphate region in the transition-state model, showing the close contact between the pentavalent phosphorous intermediate, Gly-12, Gln-61, and Tyr-32. Any amino acid other than glycine at position 12 would interfere with the position of the Gln-61 side chain.

modeled the structure of the p21(G12V) mutant in the GTP-bound conformation by replacing residues 10–17 of the GDP-[CH₂]P complex with the corresponding residues of the p21(G12V)-GDP complex. In this model, the side chain of Val-12 comes into an unfavorably close contact with the γ -phosphate and may affect the position or orientation of the γ -phosphate or the L1 region or both. More importantly, the Val-12 side chain would interfere with the intrinsic GTPase reaction by directly blocking the approach of the Gln-61 side chain in the transition state, as can be seen from Fig. 4 Lower.

Krengel *et al.* (14) report that the loop L1 conformation of the GTP complex of p21(G12V) at 2.6-Å resolution is pushed away slightly from the β - and γ -phosphates and that residues in the L4 region are also disrupted. They attribute the loss of GTPase activity to interference of the residue 12 side chain with Gln-61 and the attacking water molecule. This would not explain the effect of the Gly-12 \rightarrow Ala mutant [p21(G12A)], which also has poor GTPase activity. The alanine side-chain is probably too small to contact the Gln-61 side chain and to disrupt the preattack complex. In our transition-state model, Gln-61 comes in much closer to the α -carbon of residue 12, so that even a small side chain like that of alanine would have a blocking effect. However, neither mechanism can explain the high GTPase activity of the Gly-12 \rightarrow Pro mutant [p21(G12P)] without invoking a subtle conformational change of loop 1 by Pro-12.

Thr-59 Mutation Disrupts the Loop L4 Conformation. Retrovirus-encoded *ras* oncogenes have two activating mutations: one at the codon for amino acid 12 (glycine replaced with either serine or arginine), and the other at the codon for amino acid 59 (alanine codon replaced with a threonine codon) (29, 30). As with the position 12 and 61 mutants, the Ala-59 \rightarrow Thr mutants [p21(A59T)] have reduced GTPase activity (31–34) but are unique in that they undergo an autophosphorylation reaction in which the GTP γ -phosphate is transferred to the threonine hydroxyl group.

The crystal structures of the two nonphosphorylated Thr-59 proteins, p21(A59T) and the double mutant p21(G12V, A59T), have been solved in the GDP form, and a model of p21(G12V, A59T) in the GTP form has been built. A comparison of the GDP forms of the normal p21 and p21(G12V, A59T) mutant protein structures shows that, as with the p21(G12V) mutant, the introduction of a valine at position 12 causes practically no alterations in the surrounding protein structure. However, introduction of threonine at position 59 causes a conformational shift in residues 59 through 61 (Fig. 5) and possibly even further into the loop L4 region, where the electron density is weak. Similar changes in the 59–61 region are seen in the GDP complex of the p21(A59T) mutant structure. The conformational change results from the formation of a hydrogen bond between the threonine hydroxyl group and the main-chain carbonyl oxygen of Pro-34 in the loop L2 region. In the normal form, the Ala-59 side chain is in close contact with this region of loop L2, but in the mutant, the bulkier branched threonine side chain causes the backbone residue 59 to be pushed away from loop L2, dragging the following amino acids along with it.

In the active GTP form, our model building suggests that a p21(A59T) mutant would cause a similar perturbation in the L4 region (although the clash would probably involve different residues of loop L2 because of the conformational shift in switch II). This would move the critical Gln-61 residue away from its normal position and prevent it from stabilizing the transition state, thus reducing the GTP hydrolysis rate.

Implications for Cellular Transformation. All of these results pertain to purified p21 proteins, but their *in vivo* behavior depends on interactions with many proteins, including nucleotide exchange factors, GAP, NF1, and other unidentified effector molecules. To accurately assess the biological effect

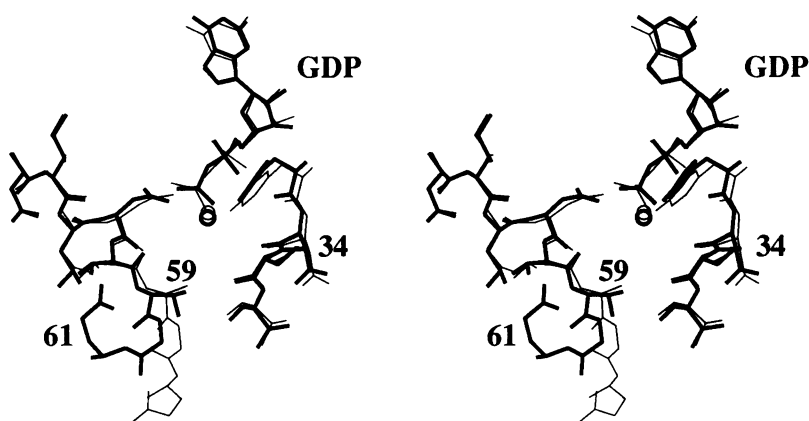


FIG. 5. Comparison of the backbone structures of the p21(G12V) (light lines) and p21(G12V, A59T) (dark lines) mutant structures in the GDP-bound states. Similar differences in the 59–61 region were seen when normal p21 (containing Gly-12 and Ala-59) and mutant p21(A59T) (containing Gly-12) were compared. The molecule in the center is the GDP, the peptide fragment on the left is made up of residues 54–61, and the fragment on the right consists of residues 32–35. The Mg^{2+} is represented by an open circle.

of these mutants from the crystal structures, the interactions between p21 and the interacting proteins must be considered. This would explain the observation that there is only a qualitative correlation between the loss of GTPase activity and transforming potential in the p21 mutants. For example, both p21(Q61E) and p21(Q61L) have the same low level of intrinsic GTPase activity; thus both exist predominantly in the GTP-bound “on” state, but only p21(Q61L) is transforming (22). This may be because the p21(Q61E) mutant interacts differently with the effector than does p21(Q61L), even though both may be in the GTP-bound form.

There appear to be two requirements for transformation potential in the GTPase-impaired mutants: (i) ability to form a complex with effector(s) and (ii) insensitivity to GTPase stimulation by GAP, NF1, or other factors. There are no known systems to date in which GAP or NF1 can restore GTPase activity to mutants that are deficient in intrinsic hydrolysis activity.

GAP binding and activity are affected by mutations in the switch I effector region (residues 30–38) and by amino acid substitutions at positions 12, 59, and 61 (4, 5, 35, 36). Furthermore, NF1 activity is blocked by p21 mutations at position 12 or 38 (7, 8). All of these residues cluster to form a patch at the surface of p21-GTP (Fig. 4 Upper), and GAP/NF1 may function in stimulating p21 GTPase activity by affecting the conformation of these residues. Because of its flexibility, the switch II region 61–64 is also a likely interaction site for GAP/NF1. These proteins may act by positioning Gln-61 so that it covers the surface patch at the γ -phosphate (Fig. 4 Lower), thus promoting formation of the transition state.

We thank Prof. N. Sakabe and Drs. A. Nakagawa and N. Watanabe of the National Laboratory of High Energy Physics, Tsukuba, Japan, for their generous help and arrangement during our synchrotron data collection and Dr. Paul Bartlett and Hyun-Ho Chung of the University of California, Berkeley, for discussions regarding the GTP hydrolysis mechanism. G.G.P. thanks the American Cancer Society, California Division, for a postdoctoral fellowship (J-15-89). This work has been supported in part by the National Institutes of Health (CA 45593), Department of Energy (Director, Office of Energy Research, Office of Biological and Environmental Research, General Life Sciences Division under Contract DE-AC03-76SF0098), and a gift to the University of California by Hoffman-La Roche and Burroughs Wellcome companies.

- Barbacid, M. (1987) *Annu. Rev. Biochem.* **56**, 779–827.
- Bos, J. L. (1989) *Cancer Res.* **49**, 4682–4689.
- Bourne, H. R., Sanders, D. A. & McCormick, F. (1990) *Nature (London)* **348**, 125–132.
- Trahey, M. & McCormick, F. (1987) *Science* **238**, 542–545.
- Vogel, U. S., Dixon, R. A. F., Schaber, M. D., Diehl, R. E., Marshall, M. S., Scolnick, E. M., Sigal, I. S. & Gibbs, J. B. (1988) *Nature (London)* **335**, 90–93.
- Trahey, M., Wong, G., Halenbeck, R., Rubinfeld, B., Martin, G. A., Ladner, M., Long, C. M., Crosier, W. J., Watt, K., Koths, K. & McCormick, F. (1988) *Science* **242**, 1697–1700.
- Martin, G. A., Viskochil, D., Bollag, G., McCabe, P. C., Crosier, W. J., Haubruck, H., Conroy, L., Clark, R., O’Connell, P., Cawthon, R. M., Innis, M. A. & McCormick, F. (1990) *Cell* **63**, 843–849.
- Xu, G., Lin, B., Tanaka, K., Dunn, D., Wood, D., Gesteland, R., White, R., Weiss, R. & Tamanoi, F. (1990) *Cell* **63**, 835–841.
- Higashi, T., Sasai, H., Suzuki, F., Miyoshi, J., Ohuchi, T., Takai, S.-I., Mori, T. & Kakunaga, T. (1990) *Proc. Natl. Acad. Sci. USA* **87**, 2409–2413.
- Milburn, M. V., Tong, L., deVos, A. M., Brünger, A., Yamaizumi, Z., Nishimura, S. & Kim, S.-H. (1990) *Science* **247**, 939–945.
- deVos, A. M., Tong, L., Milburn, M. V., Matias, P. M., Jancarik, J., Noguchi, S., Nishimura, S., Miura, K., Ohtsuka, E. & Kim, S.-H. (1988) *Science* **239**, 888–893.
- Pai, E. F., Kabsch, W., Krengel, U., Holmes, K. C., John, J. & Wittinghofer, A. (1989) *Nature (London)* **341**, 209–214.
- Pai, E. F., Krengel, U., Petsko, G. A., Goody, R. S., Kabsch, W. & Wittinghofer, A. (1990) *EMBO J.* **9**, 2351–2359.
- Krengel, U., Schlichting, I., Scherer, A., Schumann, R., Frech, M., John, J., Kabsch, W., Pai, E. F. & Wittinghofer, A. (1990) *Cell* **62**, 539–548.
- Jancarik, J., deVos, A. M., Kim, S.-H., Miura, K., Ohtsuka, E., Noguchi, S. & Nishimura, S. (1988) *J. Mol. Biol.* **200**, 205–207.
- Brünger, A. T., Milburn, M. V., Tong, L., deVos, A. M., Jancarik, J., Yamaizumi, Z., Nishimura, S., Ohtsuka, E. & Kim, S.-H. (1990) *Proc. Natl. Acad. Sci. USA* **87**, 4849–4853.
- Tong, L., deVos, A. M., Milburn, M. V. & Kim, S.-H. (1991) *J. Mol. Biol.* **217**, 503–516.
- Sakabe, N. (1983) *J. Appl. Crystallogr.* **16**, 542–547.
- Higashi, T. (1989) *J. Appl. Crystallogr.* **22**, 9–18.
- Brünger, A. T., Kuriyan, J. & Karplus, M. (1987) *Science* **235**, 458–460.
- Tronrud, D. E., Ten Eyck, L. F. & Matthews, B. W. (1987) *Acta Crystallogr. Sect. A* **43**, 489–501.
- Der, C. J., Finkel, T. & Cooper, G. M. (1986) *Cell* **44**, 167–176.
- Feuerstein, J., Goody, R. S. & Webb, M. R. (1989) *J. Biol. Chem.* **264**, 6188–6190.
- Valencia, A., Chardin, P., Wittinghofer, A. & Sander, C. (1991) *Biochemistry* **30**, 4637–4648.
- Bourne, H. R., Sanders, D. A. & McCormick, F. (1991) *Nature (London)* **349**, 117–127.
- Frech, M., John, J., Pizon, V., Chardin, P., Tavittian, A., Clark, R., McCormick, F. & Wittinghofer, A. (1990) *Science* **249**, 169–171.
- Brünger, A. T. (1990) X-PLOR 2.1, A System for Crystallography and NMR (Yale University, New Haven, CT).
- Seeburg, P. H., Colby, W. W., Capon, D. J., Goeddel, D. V. & Levinson, A. D. (1984) *Nature (London)* **312**, 71–75.
- Dhar, R., Ellis, R. W., Shih, T. Y., Oroszlan, S., Shapiro, B., Maizel, J., Lowy, D. & Scolnick, E. (1982) *Science* **217**, 934–937.
- Tsuchida, N., Ryder, T. & Ohtsubo, E. (1982) *Science* **217**, 937–939.
- Gibbs, J. B., Sigal, I. S., Poe, M. & Scolnick, E. M. (1984) *Proc. Natl. Acad. Sci. USA* **81**, 5704–5708.
- John, J., Frech, M. & Wittinghofer, A. (1988) *J. Biol. Chem.* **263**, 11792–11799.
- Feig, L. A. & Cooper, G. M. (1988) *Mol. Cell. Biol.* **8**, 2472–2478.
- Chung, H.-H., Kim, R. & Kim, S.-H. (1991) *Biochim. Biophys. Acta*, in press.
- Adari, H., Lowy, D. R., Willumsen, B. M., Der, C. J. & McCormick, F. (1988) *Science* **240**, 518–521.
- Calés, C., Hancock, J. F., Marshall, C. J. & Hall, A. (1988) *Nature (London)* **332**, 548–551.